Lattice Strain Directed Synthesis of Anatase TiO_2 Single-Crystal Microplatelet Arrays on α-MoO_3 (010) Template

Hua Gui Yang and Hua Chun Zeng*

Department of Chemical and Environmental Engineering, Faculty of Engineering, National University of Singapore, 10 Kent Ridge Crescent, Singapore 119260

Received: September 16, 2003; In Final Form: November 22, 2003

A versatile synthetic process for anatase TiO_2 microplatelet arrays has been investigated by utilizing lattice mismatches between the overlayer and the template ((010) surface of α-MoO_3). Several controlling parameters, such as organic modifiers and reactant concentrations, have also been identified for the synthesis of oriented anatase TiO_2 microplatelets and nanowires. The method developed in this work should be applicable to other oxide systems via investigating the interplay between structural resemblance and lattice mismatch.

Over the past decade, organic surfactants and molecules have been commonly used as directing templates or molecular imprints for fabrication of ordered mesoporous materials and self-assembly of low-dimensional functional materials.[1−7] Nanoparticles of metals, oxides, and semiconductors have also been prepared and organized with DNA, self-assembly monolayers (SAMs), and other organic−polymeric templates, including carbon nanotubes.[8−12] In addition to this, long-chain organic molecules with chiral centers have also been employed in synthesis to generate helical structures of oxides and sulfides.[13−15] Furthermore, organic−inorganic layered hybrids have been utilized in nanostructured metal-oxide synthesis and self-organization.[16,17] Different from these flexible "soft" molecular templates, porous host materials such as zeolites, MCM-41, and anodic alumina nanochannels are rigid "hard templates", which have been widely used nowadays for shape control of functional inorganic materials and gradient nanomaterials and composites.[18−20] Other hard templates with prefabricated patterns by the photolithography technique have also been used to grow or to organize nano building blocks.[21] Newer self-assembly methods with templating assistance such as Langmuir−Blodgett films, solvent-drying techniques, and shape-selective molds have also been developed and tested very recently.[22−24]

To explore other novel self-organizing schemes, we have recently turned our attention to epitaxial synthetic processes on single-crystal templates.[25,26] Although it has been widely used in thin-film fabrication,[27] heterogeneous epitaxial growth has not been commonly considered as a synthetic strategy for self-organization. Nonetheless, it is recognized that there exist different types of structural tensions (strains) along various crystallographic directions due to lattice mismatches between the overlayer and the substrate. This additional structural anisotropy, if properly utilized, should in principle allow one to synthesize and organize overlayer materials. Herein, to the best of our knowledge, we report a first investigation on fabrication of self-assembled micrometer-scale oxide platelet arrays by utilizing lattice mismatches between the overlayer and single-crystal substrate and resultant strain-induced reconstruction.

* Author to whom correspondence should be addressed. E-mail: chezhc@nus.edu.sg.

In our experiments summarized in Table 1, dilute hydrochloric acid solution (at pH = 2.1) was prepared from 1.5 M HCl and deionized water. Titanium tetrafluoride (TiF_4, Aldrich) was then dissolved in this solution to give a concentration of 0.040 M, during which the pH was changed to 1.8. Deionized water was used to adjust the concentration of TiF_4 to a range of 0.667−4.0 mM for hydrolysis synthesis. Chelating agent ethylenediaminetetraacetic acid disodium (EDTA salt, $C_{10}H_{14}N_2Na_2O_8 \cdot 2H_2O$, J. T. Baker) was also used as a mediate reagent. In a typical synthesis, 30 mL of the above prepared TiF_4 solution, EDTA salt, and α-MoO_3 single-crystal template (0.21 g) or α-MoO_3 nanorods (0.04−0.20 g) were added to a Teflon-lined stainless steel autoclave and heated at 160−200 °C for a period of 3−11 h. The molar ratio of TiF_4/EDTA ranged from 0.3 to 15, and the preparation of α-MoO_3 single crystals (15 mm × 2 mm × 0.5 mm) or nanorods with [010] orientation has been detailed in our previous reports.[25,26] After hydrothermal reaction, TiO_2/α-MoO_3 samples were washed with deionized water thoroughly and dried naturally at room temperature. The obtained products were characterized with scanning electron microscopy and energy-dispersive X-ray spectroscopy (SEM/EDX, JSM-5600LV), transmission electron microscopy and selected area electron diffraction (TEM/SAED, JEM-2010F, 200 kV), and X-ray diffraction (XRD, Shimadzu XRD-6000, Cu Kα radiation).[25,26] Detachment of TiO_2 products for TEM or SEM analysis was carried out with 5-min ultrasonic treatment in deionized water or by removing α-MoO_3 templates in a dilute NaOH solution.

Both α-MoO_3 and anatase TiO_2 consist of metal-centered oxygen octahedrons MO_6 (M = Mo and Ti). Because of the oxidation-state difference in the two metal ions, the octahedrons in α-MoO_3 are edge sharing along [001] and corner sharing along [100] in a layered structure (basal plane (010)) while those in anatase TiO_2 show only edge interconnectivity along all principal directions. The similarity of lattice constants between the (010) plane of orthorhombic α-MoO_3 (space group, *Pbnm*; a = 3.9630 Å, b = 13.856 Å, c = 3.6966 Å; basal spacing $d_{010}/2 = b/2$) and the (001) plane of tetragonal anatase TiO_2 (space group, $I4_1/amd$; $a = b$ = 3.7852 Å, c = 9.5139 Å) is illustrated in Figure 1. Because of the structural resemblance, it has been found that the epitaxial growth of these two surfaces can be achieved.[25,26] Nonetheless, degree of mismatch along

10.1021/jp036760o CCC: $27.50
Published on Web 12/20/2003

TABLE 1: A Brief Summary of Representative Experiments in This Work

TiF_4 (mM/mL)	with MoO_3	TiF_4/EDTA ratio	temp/time	predominant morphology
0.80/30	MoO_3 nanorods	no EDTA	200 °C/3 h	TiO_2 microplatelets (SI-5)
1.33/30	MoO_3 nanorods	3.72	160 °C/3 h	TiO_2 microplatelets (Figure 3)
2.67/30	MoO_3 plates	3.0	200 °C/3 h	TiO_2 microplatelets
2.67/30	MoO_3 plates	3.0	200 °C/6 h	TiO_2 microplatelets
2.67/30	MoO_3 plates	1.5	200 °C/6 h	TiO_2 microplatelets (Figure 2, TEM)
2.67/30	MoO_3 plates	1.5	200 °C/6 h	TiO_2 microplatelets (Figure 4, SEM)
0.67/30	MoO_3 nanorods	1.24	200 °C/3 h	TiO_2 microplatelets
1.33/30	MoO_3 plates	0.75	160 °C/11 h	TiO_2 microplatelets
2.67/30	MoO_3 plates	0.75	200 °C/3 h	TiO_2 microplatelets
1.33/30	MoO_3 plates	0.75	200 °C/6 h	TiO_2 microplatelets (Figure 4)
2.67/30	MoO_3 plates	0.75	200 °C/6 h	TiO_2 microplatelets
0.67/30	MoO_3 plates	0.372	200 °C/6 h	TiO_2 nanowires + microplatelets
0.67/30	MoO_3 plates	0.372	200 °C/3 h	TiO_2 nanowires
2.67/30	MoO_3 plates	0.3	200 °C/6 h	TiO_2 nanowires (Figure 5)
1.33/30	no	0.75	170 °C/10 h	TiO_2 crystallites (SI-3)
1.33/30	no	0.72	150 °C/25 h	TiO_2 crystallites (SI-4)
1.33/30	no	0.72	200 °C/5 h	TiO_2 crystallites (SI-4)

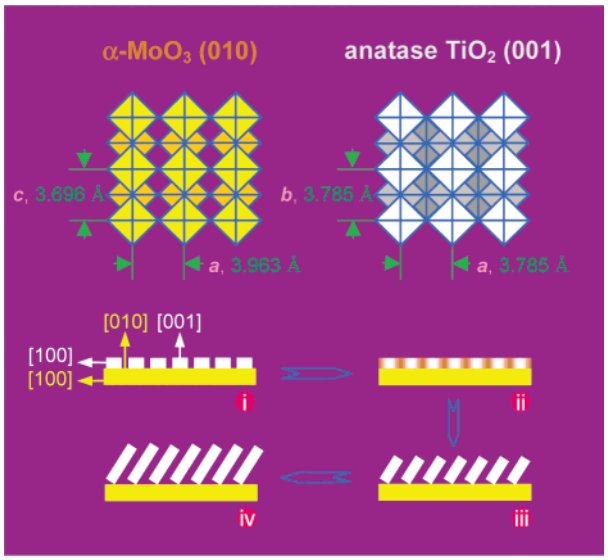

Figure 1. Structural illustrations for α-MoO_3 (viewed from [010] axis) and anatase TiO_2 (viewed from [001] axis) and a proposed mechanism for formation of TiO_2 platelet arrays (white, viewed along [010] axis) on (010) surface of α-MoO_3 (yellow, viewed along [001] axis): (i) epitaxial growth of TiO_2 islands, (ii) plane formation and strains build-up (indicated by orange colored areas), (iii) breaking along the strained lines and subsequent tilted growth, and (iv) continuous tilted growth along [100] of the microplatelets.

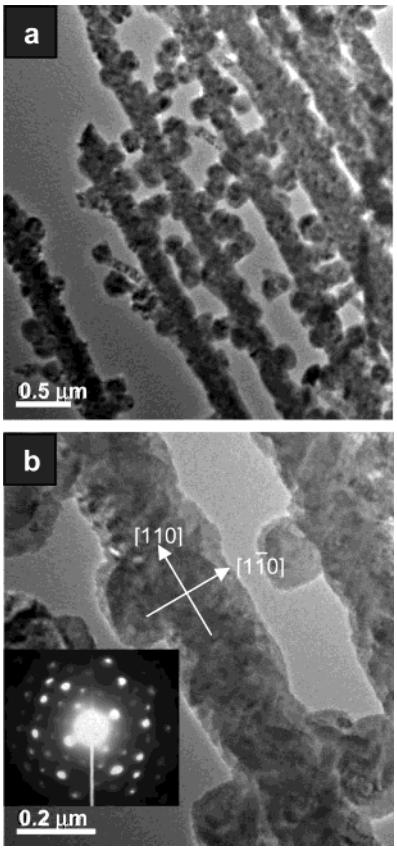

Figure 2. TEM images of detached anatase TiO_2 nanorods (separated from the α-MoO_3 (010) template): (a) parallel rods and branching (netting) and (b) a detailed view on the nanorods (inset: ED pattern of the related nanorods). Experimental conditions: $[TiF_4] = 2.67$ mM (30 mL), TiF_4/EDTA molar ratio = 1.5; at 200 °C for 6 h. The TiO_2 samples are viewed along the [001] direction.

the [100] (−4.5%) of α-MoO_3 is greater than that along the [001] (+2.4%). This lattice anisotropy was utilized in the current synthesis of TiO_2 platelet arrays, as shown in the flowchart of Figure 1.

Without using EDTA in synthesis, [001]-oriented nanospheres of anatase TiO_2 have been grown epitaxially on top of the (010) surface of α-MoO_3.[26] With the EDTA agent added in this work, the lateral growth of TiO_2, or planarization, has been promoted, which leads to the formation of flat-top islands (instead of spheres,[26] step i of Figure 1). The flat-top islands then extend horizontally and merge together forming one-dimensional lines (rodlike) and/or two-dimensional (2D) overlayers on the (010) surface of α-MoO_3. Figure 2a shows some detached TiO_2 nanorods, noting that they are interconnected forming a 2D net on the template. This rigid overlayer structure was further investigated with ED method to understand its assembly fundamentals. The ED pattern in Figure 2b can be indexed as [001] zone-diffraction spots,[25] which indicates that the anatase TiO_2 surface nets are perpendicular to the [001] direction (step i, Figure 1) and single crystalline. Furthermore, two major growth directions, approximately along [110] (Figure 2) and [100] (Figure 3), are found from the relationship between the ED patterns and nanostructures in real space. This is understandable, as most of the surface is still uncovered in the early stage of growth (i.e., unconstrained 2D expansion). With a prolonged growth, the netted nanostructures will be eventually merged and developed into a planar overlayer. Because of the nature of epitaxy, the growing planar structure of TiO_2 is still largely single crystalline. To enhance the electron-penetrating capacity for our samples, the above epitaxial growth was also investigated with thinner α-MoO_3 templates (nanorods, more transmissible to an electron beam of TEM) under the similar synthetic conditions. In Figure 3a, smaller stringlike TiO_2 arrays (nanowires) are indeed observed; these nanowires are running

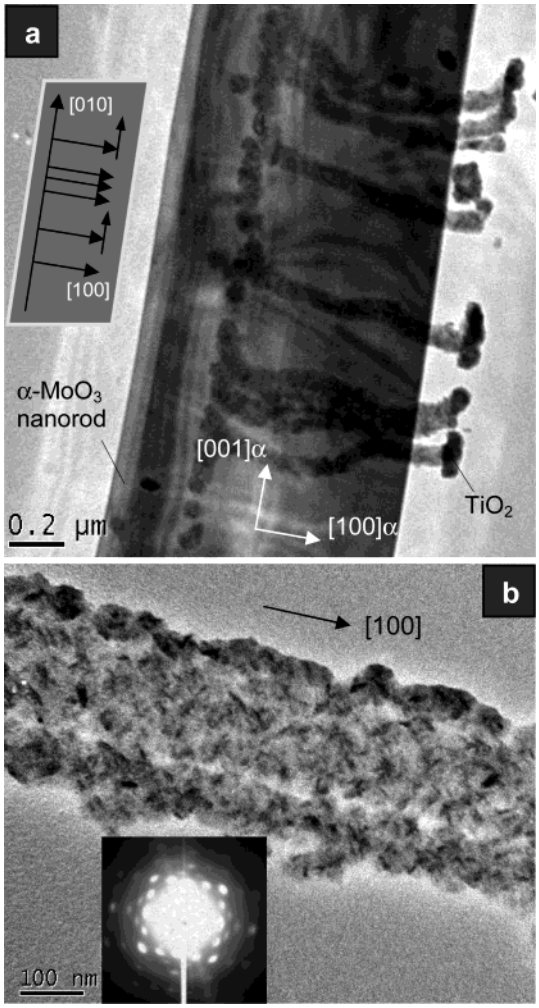

Figure 3. TEM images of anatase TiO_2 grown on α-MoO_3 nanorod template: (a) stringlike TiO_2 nanoparticles together with an α-MoO_3 nanorod template (inset indicates the growing directions of TiO_2 strings) and (b) detailed view on a detached TiO_2 overlayer (separated from the α-MoO_3 (010) template; inset: ED pattern of the related TiO_2 layer). Experimental conditions: $[TiF_4] = 1.33$ mM (30 mL), 0.05 g of α-MoO_3 nanorods, TiF_4/EDTA molar ratio = 3.72; at 160 °C for 3 h. The α-MoO_3 nanorod template is viewed along the [010] direction, while the TiO_2 is viewed along the [001].

along the [100] and [001] directions of the α-MoO_3 template, including secondary branching (small arrows, inset) at the end of the strings. Some areas of the templates are essentially covered with the TiO_2, and a detached layer fragment (i.e., a merger of these lined strings) is exampled in Figure 3b. Once again, the overlayer is essentially single crystalline with the [001] axis perpendicular to the substrate.

When the strain within a growing TiO_2 layer is accumulated up to a threshold level, cracking occurs. This process is illustrated in steps ii and iii of Figure 1. As addressed earlier, the lattice constant *a* (3.9630 Å) of the α-MoO_3 template is greater than the *a* value (3.7852 Å) of anatase TiO_2. Cracking (discontinuity) along the [100] axis of α-MoO_3 is thus expected in order to release the internal tensions of the overlayer built up during the planar growth. On the other hand, the lattice constant *c* (3.6966 Å) of α-MoO_3 is smaller than the *b* value (3.7852 Å) of TiO_2, which may initiate a self-detachment of the TiO_2 overlayer from the substrate underneath. In principle, a cooperative action of the two lattice mismatches should result in formation of elongated TiO_2 crystal strips (or platelets). The growth on the side planes of the strips continues, which can lead to a titled detachment of the TiO_2 platelets, generating a periodic platelet arrays (steps iii and iv). Figure 4 reports the resultant anatase TiO_2 platelet arrays on the (010) surface of α-MoO_3. The zigzag cracking takes place primarily along [001] and then takes a small turn along [100], forming sawtoothlike edges on crystal strips running at an angle (defined as θ) several degrees off the [001] axis of α-MoO_3. This cracking produces rectangular TiO_2 platelet strips bounded with the {100} and {010} edges and two large {001} surfaces. Continuous growth is evidenced in the [100]-oriented "sprouts" and "roots"; note that the "roots" were formed on the side toward the α-MoO_3 substrate where less nutrient was supplied from the solution. The breadth of the platelets in parts a and b of Figure 4 is about 3−5 μm, which is about half of that in parts c and d of Figure 4. This dimensional variation (and thus growth rate along [100]) can be related to the concentration changes of initial TiF_4 and EDTA salt. The platelets consist of well-crystallized submicrometer nanocrystallites, ranging from 100 to 500 nm (also refer to Figure 3). With this titled arrangement (two principal surfaces {001} per platelet) and the breadth extension, the total surface area of TiO_2 is increased significantly (>200% of the original before cracking). This synthetic strategy thus can be used to prepare ordered functional overlayer materials with a simultaneous gain in surface area. For example, the ordered surface assembly achieved in the current study is desirable for future applications as chemical sensors, as it meets all general requirements, an ordered array with a large surface area.

The XRD investigation reveals that the α-MoO_3 template did not change their orthorhombic phase after the deposition of TiO_2 (Supporting Information (SI) 1), which is in good agreement with a report that anatase TiO_2 and α-MoO_3 do not interdiffuse.[28] It is noted that there were no chemical reactions between EDTA salt and α-MoO_3 either. The anatase phase of deposited TiO_2 was also verified with our XRD study (SI 1). Furthermore, chemical compositions of TiO_2 nanowires as well as microplatelet arrays were confirmed with EDX (detected atomic ratios, Ti/O ≈ 1:2 and Mo/O ≈ 1:3, respectively, in all measured cases; SI 2).

The templating effect of α-MoO_3 is further shown in our unconstrained synthesis of TiO_2 crystallites. Under the similar synthetic conditions but without α-MoO_3, the anatase crystallites are bounded with eight {101} planes, shown as a bipyramid morphology (about 1 μm in equatorial diameter; SI 3). Elongated TiO_2 nanoplatelets with the {001} principal facets are also observed. The population of the {001} faces does increase with EDTA content and reaction temperature (SI 3 and 4), indicating a possible mediating role of EDTA salt in suppression of [001] directional growth. In contrast, by use of other organic ligands such as ethylenediamine (EDA), a crystal growth along the [001] direction can be promoted.[29] Although the exact roles of EDTA are still not totally clear at the present stage, the observed suppression may be attributed to easy coordination of EDTA (i.e., formation of ligand cages) on the (001) surface in replacing oxygen anions that are octahedrally coordinated to Ti^{4+} cations.[30] On the other hand, without adding EDTA salt, the TiO_2 overlayer on the same α-MoO_3 template was poorly crystallized (SI 5). It is concluded that the α-MoO_3 template and EDTA salt are two key synthetic parameters in this "one-pot" self-assembly process. The high versatility of this method is further demonstrated in Figure 5. When the content of EDTA is higher, only limited nucleation sites are formed on the α-MoO_3 template. In such a case, the slow reaction rate allows a predominant homogeneous growth, generating large bundles of nanowires running across the [100] direction of the template.

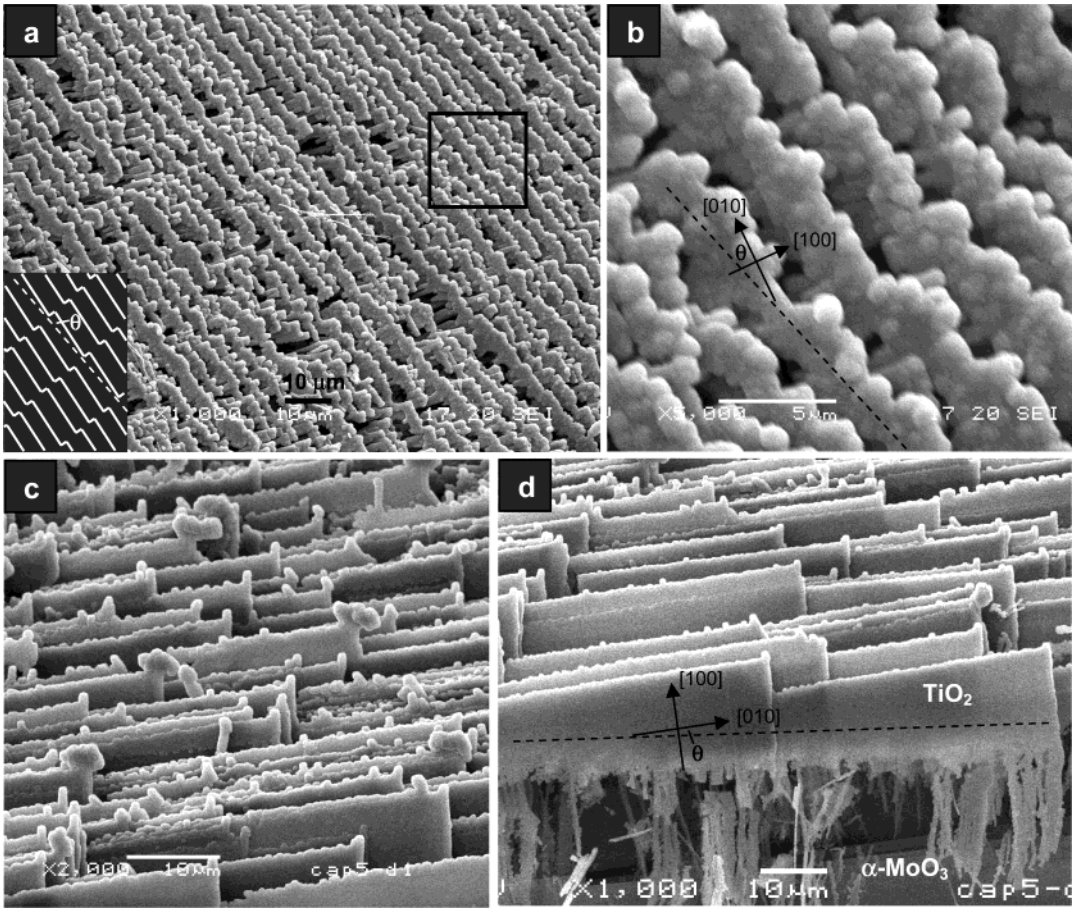

Figure 4. SEM images of anatase TiO_2 microplatelets grown on α-MoO_3 template: (a) a large scale organization of TiO_2 microplatelets (inset indicates the zigzag cracking); (b) the framed area in (a); (c) the array of TiO_2 microplatelets with a larger breadth; and (d) the "roots" the TiO_2 microplatelets of (c) toward the α-MoO_3 template. Experimental conditions: (a and b) [TiF_4] = 1.33 mM (30 mL), TiF_4/EDTA molar ratio = 0.75 and (c and d) [TiF_4] = 2.67 mM (30 mL), TiF_4/EDTA molar ratio = 1.5; all at 200 °C for 6 h. Dashed lines indicate the crystal strips directions.

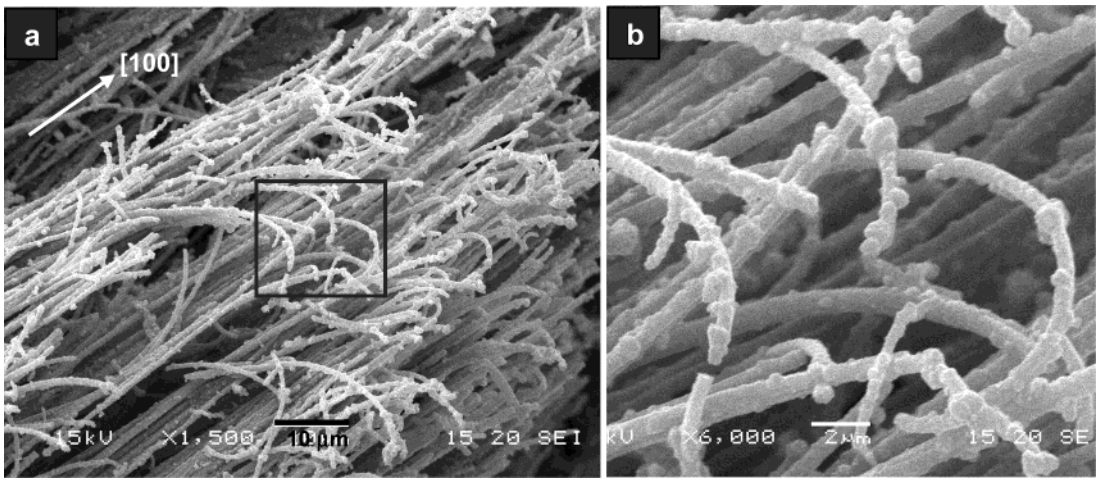

Figure 5. SEM images of anatase TiO_2 nanowires grown on α-MoO_3 template: (a) large bundles of TiO_2 nanowires grown along [100] direction of α-MoO_3 template, noting that the oxide wires are [100]-oriented and (b) the framed area in (a). Experimental conditions: [TiF_4] = 2.67 mM (30 mL), TiF_4/EDTA molar ratio = 0.3; at 200 °C for 6 h.

In summary, a versatile fabrication method of lined microplatelet arrays has been developed for the first time by utilizing lattice mismatches between the overlayer and the template. Several controlling parameters, such as organic modifiers and reactant concentrations, have also been identified for synthesis of oriented anatase TiO_2 microplatelets and nanowires. As exampled here, the synthetic method should be applicable to other oxide systems via carefully investigating the interplay between structural resemblance and lattice mismatch.

Acknowledgment. The authors gratefully acknowledge the financial support of the Ministry of Education, Singapore.

Supporting Information Available: XRD/ED patterns, EDX spectrum, and SEM/TEM images are available free of charge via the Internet at http://pubs.acs.org.

References and Notes

(1) Kresge, C. T.; Leonowicz, M. E.; Roth, W. J.; Vartuli, J. C.; Beck, J. S. *Nature* **1992**, *359*, 710.

(2) Moller, K.; Bein, T. *Chem. Mater.* **1998**, *10*, 2950.
(3) Davis, M. E. *Nature* **2002**, *417*, 813.
(4) Patzke, G. R.; Krumeich, F.; Nesper, R. *Angew. Chem., Int. Ed.* **2002**, *41*, 2446.
(5) Cölfen, H.; Mann, S. *Angew. Chem., Int. Ed.* **2003**, *42*, 2350.
(6) Xia, Y.; Yang, P.; Sun, Y.; Wu, Y.; Mayers, B.; Gates, B.; Yin, Y.; Kim, F.; Yan, H. *Adv. Mater.* **2003**, *15*, 353.
(7) (a) Rao, C. N. R.; Cheetham, A. K. *J. Mater. Chem.* **2001**, *11*, 2887. (b) Rao, C. N. R.; Kulkarni, G. U.; Thomas, P. J.; Edwards, P. P. *Chem.−Eur. J.* **2002**, *8*, 29.
(8) Alivisatos, A. P.; Johnsson, K. P.; Peng, X. G.; Wilson, T. E.; Loweth, C. J.; Bruchez, M. P.; Schultz, P. G. *Nature* **1996**, *382*, 609.
(9) (a) Aizenberg, J.; Black, A. J.; Whitesides, G. M. *Nature* **1999**, *398*, 495. (b) Travaille, A. M.; Donners, J. J. J. M.; Gerritsen, J. W.; Sommerdijk, N. A. J. M.; Nolte, R. J. M.; van Kempen, H. *Adv. Mater.* **2002**, *14*, 492.
(10) Liu, Y.; Meyer-Zaika, W.; Franzka, S.; Schmid, G.; Tsoli, M.; Kuhn, H. *Angew. Chem., Int. Ed.* **2003**, *42*, 2853.
(11) Spatz, J. P. *Angew. Chem., Int. Ed.* **2002**, *41*, 3359.
(12) Donners, J. J. J. M.; Nolte, R. J. M.; Sommerdijk, N. A. J. M. *J. Am. Chem. Soc.* **2002**, *124*, 9700.
(13) (a) Jung, J. H.; Ono, Y.; Hanabusa, K.; Shinkai, S. *J. Am. Chem. Soc.* **2000**, *122*, 5008. (b) Kobayashi, S.; Hamasaki, N.; Suzuki, M.; Kimura, M.; Shirai, H.; Hanabusa, K. *J. Am. Chem. Soc.* **2002**, *124*, 6550. (c) van Bommel, K. J. C.; Friggeri, A.; Shinkai, S. *Angew. Chem., Int. Ed.* **2003**, *42*, 980.
(14) Sone, E. D.; Zubarev, E. R.; Stupp, S. I. *Angew. Chem., Int. Ed.* **2002**, *41*, 1706.
(15) Giraldo, O.; Marquez, M.; Brock, S. L.; Suib, S. L.; Hillhouse, H.; Tsapatsis, M. *J. Am. Chem. Soc.* **2000**, *122*, 12158.
(16) Krumeich, F.; Muhr, H.-J.; Niederberger, M.; Bieri, F.; Schnyder, B.; Nesper, R. *J. Am. Chem. Soc.* **1999**, *121*, 8324.
(17) Wei, X. M.; Zeng, H. C. *J. Phys. Chem. B* **2003**, *107*, 2619.
(18) Lakshmi, B. B.; Patrissi, C. J.; Martin, C. R. *Chem. Mater.* **1997**, *9*, 2544.
(19) Nicewarner-Peña, S. R.; Freeman, R. G.; Reiss, B. D.; He, L.; Peña, D. J.; Walton, I. D.; Cromer, R.; Keating, C. D.; Natan, M. J. *Science* **2001**, *294*, 137.
(20) Sehayek, T.; Vaskevich, A.; Rubinstein, I. *J. Am. Chem. Soc.* **2003**, *125*, 4718.
(21) Kovtyukhova, N. I.; Mallouk, T. E. *Chem.−Eur. J.* **2002**, *8*, 4355.
(22) Yang, P.; Kim, F. *Chem. Phys. Chem.* **2002**, *3*, 503.
(23) Giraldo, O.; Durand, J. P.; Ramanan, H.; Laubernds, K.; Suib, S. L.; Tsapatsis, M.; Brock, S. L.; Marquez, M. *Angew. Chem., Int. Ed.* **2003**, *42*, 2905.
(24) Clark, T. D.; Ferrigno, R.; Tien, J.; Paul, K. E.; Whitesides, G. M. *J. Am. Chem. Soc.* **2002**, *124*, 5419.
(25) Lou, X. W.; Zeng, H. C. *J. Am. Chem. Soc.* **2003**, *125*, 2697.
(26) Yang, H. G.; Zeng, H. C. *Chem. Mater.* **2003**, *15*, 3113.
(27) Lange, F. F. *Science* **1996**, *273*, 903.
(28) Elder, S. H.; Cot, F. M.; Su, Y.; Heald, S. M.; Tyryshkin, A. M.; Bowman, M. K.; Gao, Y.; Joly, A. G.; Balmer, M. L.; Kolwaite, A. C.; Magrini, K. A.; Blake, D. M. *J. Am. Chem. Soc.* **2000**, *122*, 5138.
(29) Yang, H. G.; Zeng, H. C., work in progress.
(30) Liang, Y.; Gan, S.; Chambers, S. A.; Altman, E. I. *Phys. Rev. B* **2001**, *63*, 235402.